RESEARCH ARTICLE

Pyrolytic Depolymerization of Polyolefins Catalysed by Zirconium-based UiO-66 Metal-Organic Frameworks

Jerry Zhi Xiong Heng,[†][a] Tristan Tsai Yuan Tan,[†][a] Xin Li,[†][a] Wei Wei Loh,[a] Yuting Chen,[a] Zhenxiang Xing,[a] Zhiyan Lim,[a] Jennet Li Ying Ong,[b] Katherine Shiyun Lin,[b] Yusuke Nishiyama,[c] Takefumi Yoshida,[d][e] Lili Zhang[b], Ken-ichi Otake,[a][f] Susumu Kitagawa,[a][f] Xian Jun Loh,[a] Enyi Ye,[*][a] Jason Y.C. Lim[*][a][g]

[a] J. Z. X. Heng, T. T. Y. Tan, X. Li, W. W. Loh, Y. Chen, Z. Xing, Z. Lim, K. Otake, S. Kitagawa, X. J. Loh, E. Ye, J. Y.C. Lim
Laboratory for Green Porous Materials, Institute of Materials Research and Engineering (IMRE)
Agency for Science, Technology and Research (A*STAR),
2 Fusionopolis Way, Innovis #08-03, Singapore 138634, Republic of Singapore.
E-mail: jason_lim@imre.a-star.edu.sg, yeey@imre.a-star.edu.sg

[b] J. L. Y. Ong, K. S. Lin, L. Zhang,
Institute of Sustainability for Chemicals, Energy and Environment (ISCE^2)
Agency for Science, Technology and Research (A*STAR),
1 Pesek Road Jurong Island, Singapore 627833, Republic of Singapore.

[c] Y. Nishiyama,
JEOL Ltd.
Musashino, Akishima, Tokyo 196-8558, Japan

[d] T. Yoshida,
Cluster of Nanomaterials, Graduate School of Systems Engineering,
Wakayama University.
930 Sakaedani, Wakayama, 640-8510, Japan.

[e] T. Yoshida,
Physical and Chemical Research Infrastructure Group,
RIKEN SPring-8 Center, RIKEN.
Hyogo 679-5148, Japan

[f] K.-i Otake, S. Kitagawa
Institute for Integrated Cell-Material Sciences,
Kyoto University, Institute for Advanced Study, Kyoto University
Yoshida, Ushinomiya-cho, Sakyo-ku, Kyoto, 606-8501 Japan.

[g] J. Y. C. Lim
Department of Materials Science and Engineering
National University of Singapore (NUS)
9 Engineering Drive, Singapore 117576, Republic of Singapore.

Supporting information for this article is given via a link at the end of the document.

Abstract: Polyolefins such as polyethylenes and polypropylenes are the most-produced plastic waste globally, yet are difficult to convert into useful products due to their unreactivity. Pyrolysis is a practical method for large-scale treatment of mixed, contaminated plastic, allowing for their conversion into industrially-relevant petrochemicals. Metal-organic frameworks (MOFs), despite their tremendous utility in heterogenous catalysis, have been overlooked for polyolefin depolymerization due to their perceived thermal instabilities and inability of polyethylenes and polypropylenes to penetrate their pores. Herein, we demonstrate the viability of UiO-66 MOFs containing coordinatively-unsaturated zirconia nodes, as effective catalysts for pyrolysis that significantly enhances the yields of valuable liquid and gas hydrocarbons, whilst halving the amounts of residual solids produced. Reactions occur on the Lewis-acidic UiO-66 zirconia nodes, without the need for noble metals, and yields aliphatic product distributions distinctly different from the aromatic-rich hydrocarbons from zeolite catalysis. We also demonstrate the first unambiguous characterization of polyolefin penetration into UiO-66 pores at pyrolytic temperatures, allowing access to the abundant Zr-oxo nodes within the MOF interior for efficient C-C cleavage. Our work highlights the potential of MOFs as highly-designable heterogeneous catalysts for depolymerisation of plastics which can complement conventional catalysts in reactivity.

Introduction

Plastics, while indispensable in modern society, have become a tremendous environmental issue from the waste they generate, particularly in the form of single-use polyolefins.[1] Comprising of

polyethylenes (PEs) and polypropylenes (PPs), polyolefins constitute the single largest family of plastics produced and disposed of today.[2] Current recycling methods are largely inadequate: other than very low rates of polyolefin recycling, mechanical recycling has stringent requirements for plastic waste sorting and causes unavoidable polymer degradation,[3] highlighting the need for alternative end-of-life strategies.[4,5,6] However, depolymerization of polyolefins is hampered by their inertness, owing to the lack of labile linkages (e.g. esters, carbonates) along their backbones. Amongst various techniques, pyrolysis is particularly noteworthy for its ability to handle a diverse range of feedstocks,[5,6] and is a practical technology for depolymerization of plastics performed on industrial scales today.[7] Pyrolysis involves heating plastics in an oxygen-free environment, typically between 400–900 °C, transforming them into lower molecular weight hydrocarbons. These products can then be further refined and used as fuels, or further chemically transformed into other valuable materials.[8,9]

Catalysts are vital in enhancing pyrolysis efficiency to produce practically-useful yields of the more valuable liquid and gaseous fractions. While acidic zeolites have been conventional choices for polyolefin pyrolysis,[10–16] there is growing interest in using polymerization catalysts to facilitate polymer deconstruction.[17–19] These catalysts lower the energy barriers for both the forward polymerization and reverse bond-breaking reactions. Leveraging established reaction mechanisms thus enables direct application of extensive knowledge from forward polymerisation catalysis for depolymerisation. Specifically for polyolefins, zirconium species which resemble Ziegler-Natta catalysts have been shown to facilitate polyethylene chain cleavage.[17–22] The C-C bond breaking step is proposed to proceed via β-alkyl elimination, the reverse step of migratory insertion (**Figure 1a**).[17–22] This offers an interesting alternative to the conventional mechanism of carbocation generation and random rearrangements when acidic zeolites are used as catalyst.[10,11,23]

As heterogeneous catalysis, metal-organic frameworks (MOFs) have proven to be exceptional owing to their chemical designability and large internal surface areas,[24,25] but have largely been overlooked in the field of plastic depolymerization. MOFs offer even greater porosities than zeolites and have been extensively studied as catalysts for forward polymerization reactions (**Figure 1b**),[25–28] suggesting their untapped potential for depolymerization. In addition, compared to completely inorganic heterogeneous catalysts employed for pyrolysis,[29] the concept of isoreticular synthesis allows for precise bottom up design and tuning of the catalytically-active sites and pore sizes to achieve targeted reactivity.[30] Despite these advantageous characteristics of MOFs in heterogenous catalysis, their perceived thermal instability compared to inorganic materials has precluded their applications in pyrolysis. Even the most thermally stable MOFs decompose at temperatures around 500 °C,[31] which is a typical polymer pyrolysis temperature. Furthermore, there is a prevailing view that the low diffusivity of high molecular weight polymers prevents their entry into MOF pores from the melt,[32] with the exceptions of PEG and some low molecular weight polymers.[33,34] Nearly all other examples of polymers within MOF pores involve the infiltration of the monomer followed by polymerization inside the pores.[32,35] To the best of our knowledge, only two examples of MOFs catalysing polymer degradation have been reported. Farha and coworkers demonstrated that zirconium MOFs facilitated the breakdown of polyethylene terephthalate (PET) at 260 °C,[36] and Manna and coworkers employed ruthenium hydride species supported in zirconium MOFs for shape-selective hydrogenolysis of polyolefins at 200 °C.[37]

Herein, we demonstrate that UiO-66,[38,39] a benchmark zirconium MOF, can be effective catalysts for polyolefin pyrolysis, enabling significantly enhanced liquid and gas yields whilst suppressing unproductive char formation. UiO-66 possessed several properties ideal for polyolefin pyrolysis: Given that zirconium metal sites in MOFs can catalyse ethylene polymerization (**Figure 1c**),[26,27] the unsaturated sites on defective UiO-66 are expected to facilitate the reverse C-C bond breaking at elevated temperatures (**Figure 1a**). The nodes of zirconium MOFs dehydrate at temperatures above 300 °C and lose acidic protons,[24,40] limiting protolytic pathways for polyethylene cleavage. In contrast to Brønsted-acidic zeolites such as HZSM-5 which often affords high aromatic production,[10–13] we show that the proposed β-alkyl elimination mechanism for UiO-66 offers complementary reactivity to yield more short-chain alkanes and terminal olefins. Furthermore, UiO-66 is notable for its excellent chemical stability,[39] ease of preparation and the potential for scalable synthesis in high yields using inexpensive terephthalic acid.[41] UiO-66 is also known to be stable up to 450 °C.[31] Although this is lower than the typical pyrolysis temperature, we hypothesize that the reactivity of the unsaturated Zr nodes can lower the required pyrolysis temperatures. Thus, utilizing MOFs facilitates the easy synthesis of coordinatively-unsaturated nano-sized zirconium-oxo species, whose catalytic activity is maintained by the rigid scaffold of the MOF, preventing aggregation which would attenuate their reactivity.[24] Finally, with UiO-66 possessing larger pore windows (6-7 Å)[39] than the well-studied polyethylene pyrolysis catalyst HZSM-5 (5.5 Å),[14,16] polyethylenes are anticipated to enter UiO-66 under similar conditions. Indeed, a combination of thermal and spectroscopic studies indicate that polyolefins can diffuse into the MOF at pyrolytic temperatures, thus allowing full utilization of the UiO-66's high internal surface area for depolymerisation mediated by its zirconium nodes. Furthermore, we show that the UiO-66 catalysts can withstand the pyrolysis reaction conditions for repeated reuse. Our studies spotlights the untapped possibilities of MOFs as practical and easily-handled unconventional catalyst for pyrolysis, opening new avenues in end-of-life plastic treatment.

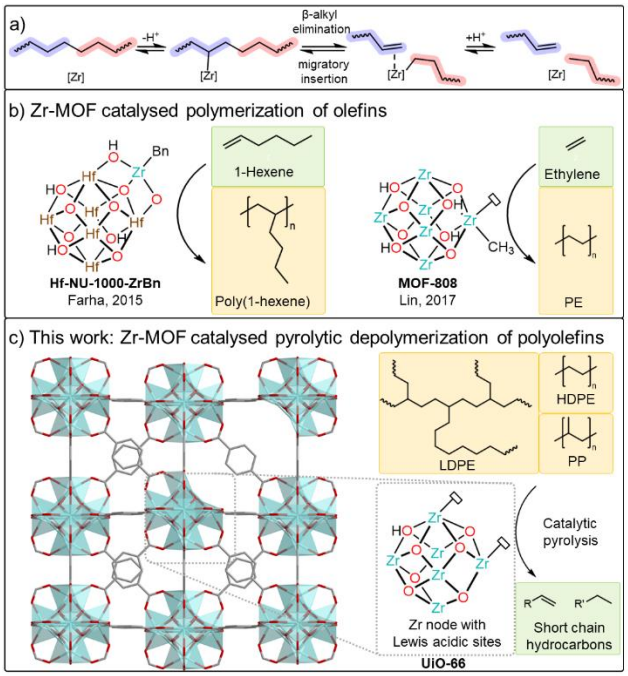

Figure 1. a) Proposed mechanism for Zr-catalysed C-C bond cleavage in polyethylene, representing the reverse step of olefin polymerization. b) Schematic illustration of prior work using Zr(IV) sites in MOF for olefin polymerization. c) Schematic illustration of this work, showing the structure of UiO-66, highlighting missing linker defects and unsaturated Zr sites which can be used for catalytic pyrolysis of polyolefins.

Results and Discussion

Pyrolysis Of Polyolefins Catalysed By UiO-66.

The UiO-66, as synthesised following reported procedures,[41] was first activated by heating in a furnace at 300 °C for an hour to completely remove any remaining formate ligands, and its crystallinity was confirmed by XRD analyses (Figure S1). The number of missing linker defects was determined by thermogravimetric analysis (TGA) as first reported by Shearer and coworkers,[42] revealing an average of 1.3 missing terephthalate linkers per Zr_6 node in the activated samples (Figure S10). These Lewis acidic sites are essential as catalytic centres for polyolefin pyrolysis. Additionally, TGA showed that significant UiO-66 decomposition occurred only above 450 °C (Figure S10), corroborating earlier reports,[39,40] and hence pyrolysis was performed at 400 °C on the lab-scale (Figure S15). UiO-66-catalysed polyolefin pyrolysis was first investigated using 2 g (71.4 mmol repeating ethylene units) of high molecular weight high-density polyethylene (HDPE) resins (M_n = 14 kDa; M_w = 186 kDa). After 5 hours, the UiO-66 (10 wt%)-catalysed reaction yielded small amounts of remnant solids, comprising of char and partially-pyrolyzed PE, and significant quantities of a liquid fraction that was collected as a clear yellow oil. Compared with the uncatalyzed control experiment (Table 1, entry 1), UiO-66 significantly enhanced conversions and yields of liquid and gaseous products while concomitantly reducing solid char formation by nearly 50% (entry 2). This indicates a more efficient cleavage of HDPE into smaller molecular fragments in the presence of UiO-66. When UiO-66 was substituted with commercially available ZrO_2 microparticles (see Figure S5 for XRD characterisation), there was an unexpected reduction in conversion compared to the uncatalyzed reaction, with a predominant portion of the HDPE substrate persisting as solid wax (entry 3). We hypothesized that poor performance of the micron-sized ZrO_2 are due particle agglomeration and suboptimal surface properties, which could impede effective mass transfer of HDPE and its access to catalytic sites. The stability of the nano-sized clusters afforded by the rigid MOF structure is therefore crucial in maintaining good catalytic activity.

Encouraged by these results, we extended our study to low-density polyethylene (LDPE) and polypropylene (PP) resins. Like HDPE, UiO-66 considerably improved conversion, liquid and gas yields from LDPE compared to the uncatalyzed reaction and with ZrO_2 (Table 1). With PP, UiO-66 also improved liquid yields, decreased solid residue formation and increased overall conversion, though to a more modest extent, as the uncatalyzed reaction already showed high conversion attributing to the lower thermal stability of PP.[43] The PE conversions in the presence of UiO-66 catalysts, achieving 44-50% yields of liquid products, are on par with the performance of zeolite catalyst.[10,11] Notably our experiments were conducted at a lower temperature of 400 °C, whereas conventional zeolite catalysts typically require higher temperatures in the range of 500-700 °C for similar conversions.[10,11]

Following this, we explored the practicality of UiO-66 in pyrolysis of real-world post-consumer LDPE and HDPE waste in the form of LDPE foam and HDPE detergent bottles respectively (entries 9, 10). In both cases, conversions exceeding 70% with comparable liquid yields as PE resins were obtained, while uncatalyzed pyrolysis of post-consumer LDPE and HDPE resulted in 32 % and 47 % conversion respectively (Table S1 entries S1 and S2), further corroborating UiO-66's value for converting post-consumer polyolefinic waste into diverse hydrocarbon products.

Liquid product distribution analysis for both $LDPE_{UiO-66}$ and $HDPE_{UiO-66}$ revealed considerable differences from their uncatalyzed reactions (**Figure 2**). While HDPE still yielded mainly linear alkanes as the major product with UiO-66 present, there was a considerable increase in linear olefin content, with a concomitant reduction in cyclic alkanes and olefins formed. The increase in linear products without any increase in branched or cyclic products formed is likely due to suppression of free radical pathways in the presence of UiO-66 and therefore a reduction in rearrangement reactions of the mainly linear polyethylene chains. For LDPE, there was a similar increase of linear alkane and olefin production, as well as an unexpected increase in cyclic alkane production. A greater proportion of cyclic alkanes was also observed in the PP_{UiO-66} reaction compared to the uncatalyzed reaction (Figure S20). Notably, UiO-66 catalysis afforded minor aromatic production for all three polyolefins (their presence confirmed by ^{1}H NMR in Figures S18), which were absent in the uncatalyzed reactions (Figure S19). The aromatic yield with UiO-66 was lower compared to using ZSM-5 catalysts,[10,11] aligning with our aforementioned proposed mechanism. However, the fact that aromatics are produced at all strongly indicates that the zirconium nodes are indeed behaving as acidic catalyst, and also suggests the accessibility of alternative reactions pathways during pyrolysis, such as carbocation generation through hydride abstraction.

Table 1. Summary of reaction conditions for pyrolysis of polyolefins.[a]

Entry	Substrate	Catalyst	Conversion [b] (%)	Fraction Yields [b]		
				Solid (%)	Liquid (%)	Gas (%)
1	HDPE	-	57.3 ± 0.9	42.7 ± 0.9	38.5 ± 6.8	18.8 ± 5.9
2	HDPE	UiO-66	80.7 ± 0.2	19.3 ± 0.2	51 ± 3.4	29.7 ± 3.6
3	HDPE	ZrO_2[c]	41.9 ± 8.8	58.1 ± 8.8	21.9 ± 0.9	20.0 ± 9.6
4	LDPE	-	51.2 ± 8.4	48.8 ± 8.4	28.3± 4.7	23.1 ± 5.1
5	LDPE	UiO-66	76.9 ± 3.1	23.1 ± 3.1	44.4 ± 9.5	32.4 ± 6.4
6	LDPE	ZrO_2[c]	68.4 ± 1.8	31.6 ± 1.8	49.5 ± 2.6	18.9 ± 0.7
7	PP	-	91.6 ± 6.5	8.4 ± 6.5	67.3 ± 9.8	24.3 ± 3.3
8	PP	UiO-66	97.8 ± 0.1	2.2 ± 0.1	76.1 ± 1.4	21.6 ± 1.3
9	HDPE waste	UiO-66	70.7 ± 7.5	29.3 ± 7.5	45.4 ± 1	25.3 ± 6.5
10	LDPE waste	UiO-66	73.2 ± 4.3	26.8 ± 4.3	49.1 ± 5.9	24.1 ± 1.6
11	HDPE[d]	-	53.9 ± 1.4	46.1 ± 1.4	26.9 ± 1.7	27 ± 0.3
12	HDPE[d]	UiO-66	68.9 ± 0.4	31.1 ± 0.4	46.6 ± 5	22.4 ± 4.7
13	LDPE[d]	-	48.3 ± 14.1	51.7 ± 14.1	24.3 ± 19.7	24 ± 5.6
14	LDPE[d]	UiO-66	74.8 ± 1.8	25.2 ± 1.8	43.8 ± 3.1	31 ± 4.8

[a] Reaction conditions: 10 wt% catalyst loading w.r.t. substrate, 400 °C for 5 hours with a constant stir rate of 150 RPM. Commercially available resins and a lab-scale pyrolysis set-up (Figure S15) are used unless otherwise stated; [b] Determined from the average of two repeat experiments, see Experimental Section for details of calculations; [c] Monoclinic ZrO_2 microparticles (Figure S5) were purchased from commercial sources; [d] Reactions performed using a fixed bed reactor (Figure S16) at 400 °C for 5 hours under constant N_2 flow.

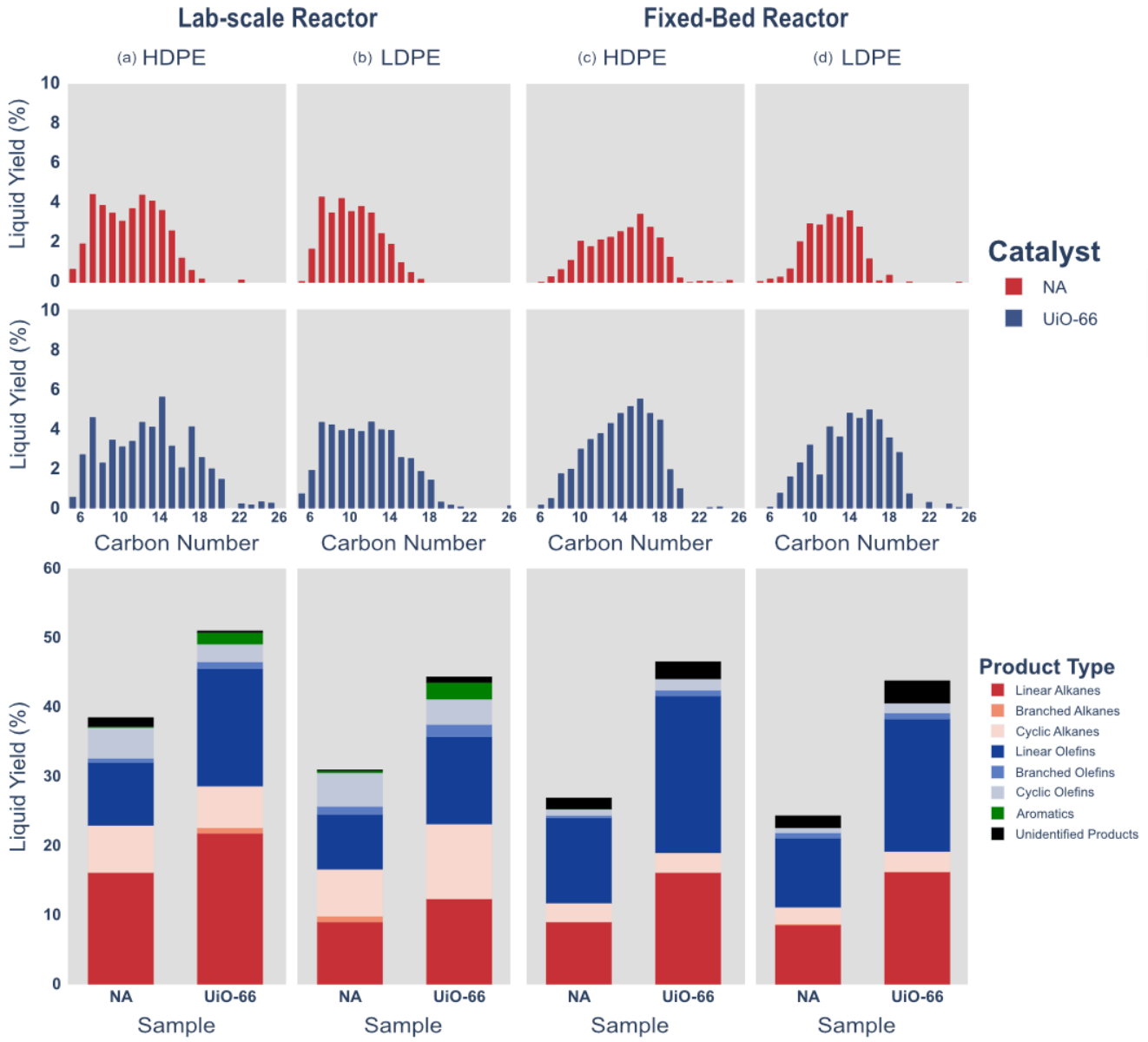

Figure 2: Comparisons of the carbon numbers and product type distributions in the pyrolysis oil fractions for reactions performed in the presence and absence of UiO-66 in the lab scale setup for (a) HDPE and (b) LDPE, and in the fixed bed reactor for (c) HDPE and (d) LDPE.

Analysis of the carbon number distribution of the liquid hydrocarbon fractions obtained from UiO-66-catalysed PE pyrolysis, using our lab-scale reactor, generally resulted in slightly broader distributions compared to the uncatalyzed control reactions (Figure 2). Greater quantities of higher molecular weight (>C18) oligomers were formed in the presence of the MOF. Notably, the distribution obtained was also broader than that obtained from PE hydrogenolysis catalysed by ruthenium-hydride-containing UiO-66 MOFs as reported by Manna and coworkers.[37] Notwithstanding the fact that hydrogenolysis is a distinctly different reaction from pyrolysis, the effect of the pore size of the MOF on the carbon number distribution of the pyrolysis oil should still be comparable. We attributed the observed differences to the smaller pore size after Ru metalation of the UiO-66,[37] as well as the defective nature of the UiO-66 used in our study resulting in a slightly larger pore size than in the defect free MOF.

To determine the stability of the UiO-66 catalyst under pyrolytic conditions, the MOF-containing post-pyrolysis residue was characterised by XRD and transmission electron microscopy (TEM). XRD revealed that while some residual amorphous post-pyrolyzed polyolefin material is present, the diffraction peaks of UiO-66 were clearly observable and showed minimal changes (**Figure 3a**). Notably, the lack of observable peak broadening indicated negligible changes in crystallite size, and the absence of new peaks suggested that no phase transition occurred,

despite the possibility of UiO-66 converting to MIL-140 at elevated temperatures.[36] These were corroborated by TEM imaging (**Figure 3b**), which showed that the MOFs largely retained their octahedral morphology, without observable formation of rodlike MIL-140. The absence of a phase change can be attributed to the non-polar nature of molten polyethylene, which is unable to facilitate the phase transition between UiO-66 and MIL-140 that likely involves charge-separated intermediates, possibly through framework disassembly and reassembly.[36] In addition, synchrotron XRD and X-ray absorption fine structure (XAFS) measurements of UiO-66 post pyrolysis were performed to detect if any ZrO_2 was formed from decomposition of UiO-66 (Figures S13 and S14). No ZrO_2 could be detected by both these methods, further supporting that UiO-66 retained its crystallinity throughout the pyrolysis process. It is important to note that maintaining temperature stability during the pyrolysis reaction is critical for UiO-66 to remain viable, which is essential for achieving good yields. Temperature spikes caused by the thermostat not being immersed in the plastic led to UiO-66 decomposition and consequently poorer yields.

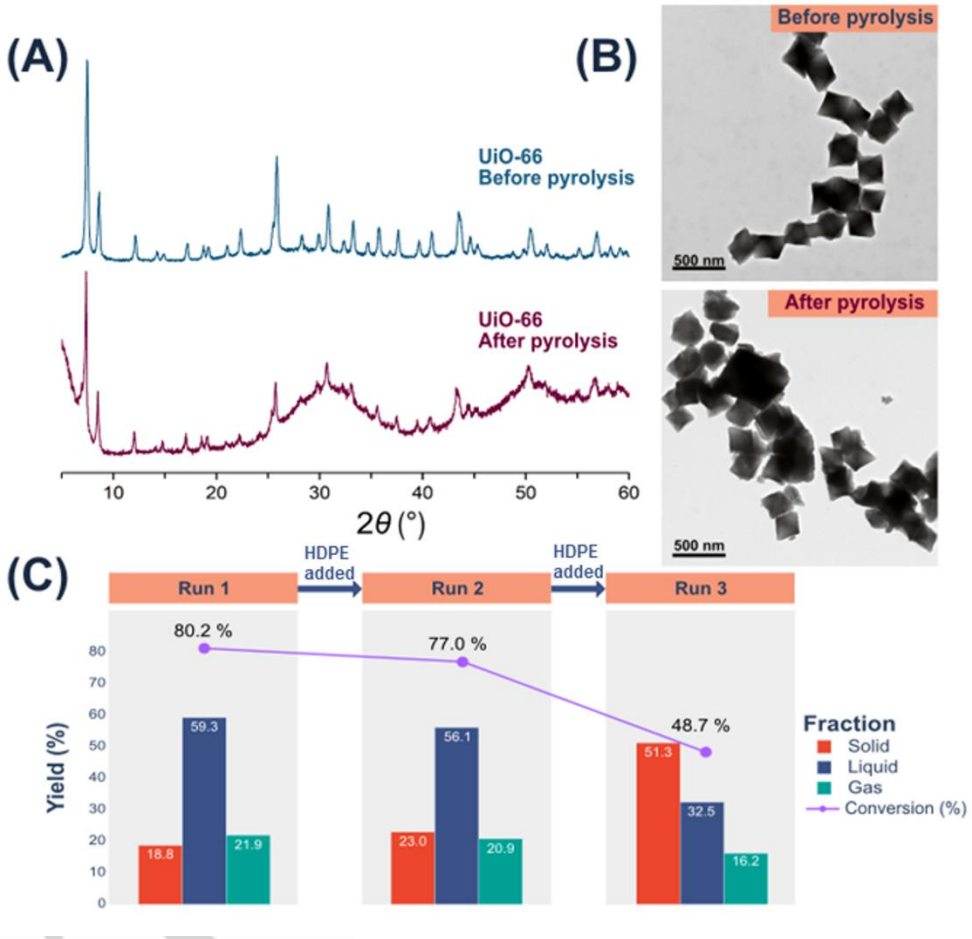

Figure 3: (a) XRD patterns of UiO-66 before pyrolysis (top) and post-pyrolysis residue (bottom), indicating presence of crystalline UiO-66 remaining in the residue; (b) TEM images of UiO-66 (top) before and (bottom) after pyrolysis; (c) MOF reusability experiments with successive HDPE pyrolysis runs.

With the thermal robustness of UiO-66 for pyrolysis established, we investigated the possibility of reusing them for successive HDPE pyrolysis runs. Other than the reaction vessel, the rest of the pyrolysis setup was thoroughly cleaned prior to additions of new batches of HDPE for reruns. As summarized in **Figure 3c**, reusing the post-pyrolysis MOFs once (run 2) resulted in slight lower, but comparable conversion and liquid yield compared to pristine UiO-66 catalysis (run 1). However, pyrolysis efficacy reverted to near-uncatalyzed conditions (Table 1) upon reusing the MOFs a second time (run 3). TEM imaging revealed that the UiO-66 maintained its morphology for two runs but showed significant residue accumulation and structural changes by the third, likely causing decreased catalytic activity (Figure S8). In addition, N_2 absorption isotherm measurements of the post pyrolysis UiO-66 (Figure S12) reveal a lack of porosity, likely due to wax and char accumulating in the MOF. These findings also demonstrate that retaining the integrity and porosity of UiO-66 MOFs was essential for its observed catalytic properties, and that coked or thermally degraded of UiO-66 were not catalytically active. The reactivation or recycling of UiO-66 would be a valuable direction for further investigation.

We then explored the possibility of UiO-66 catalysing LDPE and HDPE pyrolysis using a practical fixed-bed reactor set-up under constant N_2 flow, equipped with on-line GC-TCD-FID analysis, to explore the influence of different reactor set-ups on polyethylene pyrolysis. Corroborating our lab-scale experiments, UiO-66 catalysis using the fixed-bed reactor consistently afforded increased conversion and liquid yields for HDPE and LDPE (Table

1, entries 12-15). However, unlike lab-scale experiments which yielded bimodal or trimodal product distributions, fixed-bed pyrolysis afforded unimodal distributions for both HDPE and LDPE irrespective of UiO-66's presence (Figure 2). For HDPE, both the UiO-66-catalyzed and uncatalyzed reactions afforded left-skewed distributions peaking at C16; whilst for LDPE, UiO-66 catalysis resulted in slightly longer products (C14-16 peaks) than its uncatalyzed counterpart (peak at C12). Evaluating the product type distribution revealed that both HDPE and LDPE predominantly yield linear alkanes and olefins, with a minor fraction of branched hydrocarbons. In addition, LDPE pyrolysis yielded a higher production of C1-4 gases, possibly due to its branched structure that facilitates polymer breakdown, while HDPE favoured C2-3 hydrocarbon production (Table S11). Notably, aromatic compounds were conspicuously absent under these conditions. We hypothesised that a consistent nitrogen flow in the fixed-bed reactor precludes the recirculation of gaseous intermediates within the reaction vessel for secondary reactions such as intramolecular cyclization and dehydrogenation to occur. The absence of aromatics produced herein also indicated that those observed in the lab-scale set-up (Figure 2) were not produced from degradation of the UiO-66's terephthalate ligands.

Finally, UiO-66 samples containing fewer defects were synthesized using the procedure reported by Shearer and coworkers[44] and used for LDPE pyrolysis to test our hypothesis that the Lewis acidic defects were indeed the catalytic sites. In line with our expectations, UiO-66 containing 0.75 missing linkers per Zr_6 node yielded a lower conversion of 60.3% (Table S1, Entry S3), compared to UiO-66 containing 1.6 missing linkers per node (76.9%, Table 1, Entry 5), while still being higher than the uncatalyzed pyrolysis of LDPE (51.2%, Table 1, Entry 4).

Mechanistic Studies

A series of further investigations were conducted to gain insight into the reaction mechanism of polyolefin pyrolysis catalysed by UiO-66. Importantly, we sought to determine whether interactions between the plastics and the zirconium nodes was limited to the external surface of MOF crystals, or if the polymers could enter the porous framework and react within its interior (as illustrated in **Figure 4a**). To this end, we first employed differential scanning calorimetry (DSC), as first demonstrated by Uemura and coworkers,[34] to investigate the ability of polyethylene to infiltration into UiO-66 at elevated temperatures. Because polymers confined in the MOF pores do not contribute to the heat of phase transitions measured for the bulk polymer, the measured enthalpies per cycle indicates the quantity of bulk polymers outside the MOF pores and thus indirectly reflect the quantity of polymer that has entered the MOF pores. Thus, a physical mixture of activated UiO-66 and HDPE was first heated to 200 °C, which allowed for the polymer to melt but was well below the pyrolysis temperature, and held for 15 minutes to allow polymer infiltration into the MOF. Subsequent heating and cooling cycles of HDPE with UiO-66 revealed successive decreases in heat change associated with both melting and crystallization (**Figure 4b**), confirming HDPE's infiltration into the MOF structure when molten. Notably, this behaviour was not observed when identical DSC experiments were performed in the absence of UiO-66 (Figure S24). Although more pronounced polymer infiltration is expected closer to pyrolysis temperatures (400 °C), such temperatures were not feasible using DSC. In contrast, the highly branched LDPE did not exhibit this behaviour (see Figure S22). While this suggests that LDPE may not readily enter UiO-66's pores due to steric hindrance, we postulate that the more readily-cleaved branch points of LDPE[5] enable it to first react on the surface of UiO-66, fragmenting into shorter less-branched chains which could then enter the pores and undergo further reaction. Indeed, DSC penetration experiments using eicosane ($C_{20}H_{42}$) confirmed the possibility of PE oligomers entering the MOF pores (Figure S25). In addition, the linear tips of branched LDPE are known to infiltrate into HZSM-5,[14] which has smaller pores than UiO-66 (~5.5 Å for HZSM-5,[14] 6-7 Å for UiO-66[39]). Hence, while our DSC experiments show that the bulk polymer cannot infiltrate UiO-66, we postulate that the linear tips can still access the internal catalytic sites of the MOF. Similar to LDPE, repeated heating and cooling cycles of isotactic PP resin with UiO-66 showed negligible changes in heat of melting and crystallization, indicating that isotactic PP is sterically too large to infiltrate the pores of UiO-66 (Figure S23) at 200 °C. We postulate that the coiled structure of isotactic PP prevents it from entering the pores of UiO-66,[45] and is also known to not penetrate HZSM-5.[15]

At higher temperatures closer to that of pyrolysis, the expected greater mobility of the polymers and flexibility of the UiO-66 framework motivated us to employ a series of solid-state NMR techniques to provide further evidence of polyolefin penetration into the MOF. After annealing a mixture of HDPE and UiO-66 at 350 °C under a nitrogen atmosphere for two hours (see Section S5), the ^{1}H 2D spin-exchange NMR (^{1}H SQ / ^{1}H SQ homonuclear correlations) spectrum of the mixture clearly revealed a cross peak indicating intermolecular interactions between the polymer and the ligand of the MOF (**Figure 4c**). Assuming a spin diffusion coefficient of 0.8 nm^2/ms,[46] mixing time of 50 ms allows spin diffusion across 6 nm, allowing us to conclude that HDPE chains are located within 6 nm from UiO-66 linkers. To further validate the close proximity of the polymer to the ligand of the MOF, 2D ^{1}H DQ / ^{1}H SQ homonuclear correlations NMR was conducted. Weak but clear correlations between polymer and ligand were also observed (Figure S26). Since ^{1}H DQ correlation can only be made between ^{1}Hs within 4 Å, the correlation indicates proximities on an atomic (< 4 Å) scale. Presence of correlation peaks in ^{1}H SQ/^{1}H SQ spectra at a short contact time of 5 ms also corroborates this observation (Figure S27). Surprisingly, 2D NMR experiments revealed correlations between the protons on PP and UiO-66, suggesting that PP could also penetrate into the MOF after heating to 350 °C (Figures S26, S27). We hypothesized that at this temperature, either increased UiO-66 flexibility permitted PP penetration, or some PP

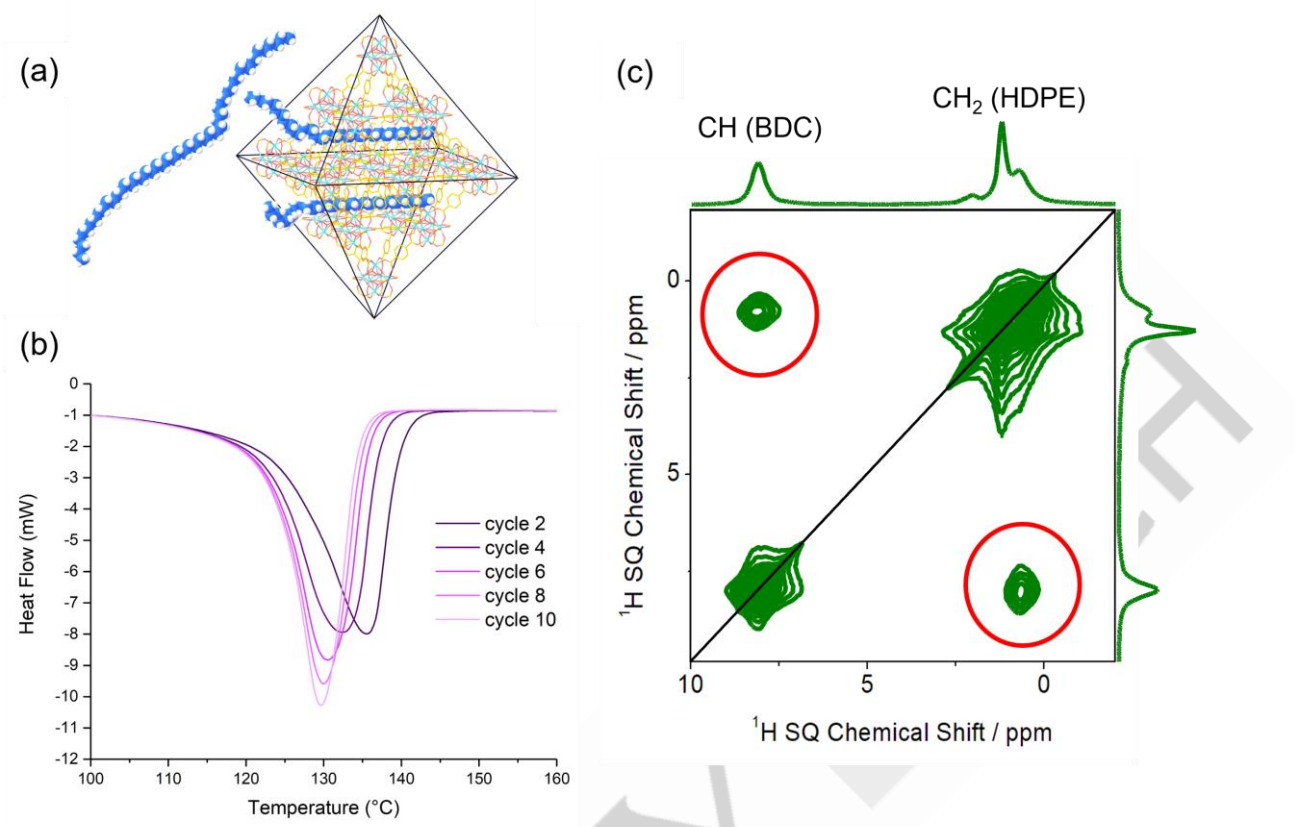

Figure 4. a) Illustration of HDPE strand infiltration into UiO-66 pore, b) DSC thermogram of the UiO-66 mixture with HDPE, showing decreasing polymer melting heat during successive heating cycles, c) ^{1}H 2D spin-exchange NMR spectrum (1H SQ / 1H SQ homonuclear correlations) of UiO-66 and HDPE after heating to 350 °C. The spectrum was observed with a mixing time of 50 ms. Correlations between HDPE and linker of UiO-66 is highlighted by circled crosspeaks in (c).

fragmentation into shorter oligomers has occurred, causing the polymer to lose its coiled structure for easier pore entry.

We then sought to understand how UiO-66 catalysts significantly improved liquid and gaseous yields for polyethylene pyrolysis - a desirable outcome considering their higher value over solid wax and char. Uncatalyzed pyrolysis typically occurs via radical mechanisms,[5,47,48] with an increased likelihood of radical recombination and cross-linking at lower temperatures.[5,48,49] This accounts for the significant wax formation in the uncatalyzed reactions, and why higher temperatures are needed to achieve satisfactory liquid yields. While our original hypothesis that unsaturated sites on the zirconium nodes could facilitate C-C bond cleavage through β-alkyl elimination would preclude the possibility for crosslinking, other ionic pathways enabled by the MOF could also be contributing. In addition, the presence of non-negligible amounts of aromatics in the product suggest that dehydrogenation pathways, possibly via β-hydride elimination, are also accessible.

To assess the feasibility of our hypothesized mechanism, we performed computational modelling using *n*-decane to model a segment of polyethylene and a truncated cluster model of UiO-66 using ORCA 5.[50] One plausible pathway is discussed herein and illustrated in **Figure 5a** (see Section S6 for full computational details and additional modelling). Drawing inspiration from the work of Van Speybroeck and coworkers,[40] we first investigated if the C-H bonds of our model hydrocarbon could be cleaved heterolytically over the amphoteric UiO-66 node, where the μ_3-oxo could act as a base. A concerted metalation-deprotonation via a 4 membered transition state (**TS1**, with an energy reaction barrier of 18.9 kcal/mol) would yield a zirconium alkyl complex. While a typical monometallic-centred β-carbon elimination transition state could be found with an overall barrier of 65.1 kcal/mol, a lower-energy bimetallic transition state (**TS2**, 57.6 kcal/mol) was also found, where an adjacent Zr atom on the node offered an empty coordination site (see Section S6 for details on both transition states). This transition state would be rate-limiting, but still below the homolytic C-C bond dissociation energy.[8,51] We estimate that the β-carbon elimination barrier in the actual system might be lower than in our model system, as C-C bonds are known to be more prone to cleavage as chain length increases.[51] Furthermore, nodes bearing more than one missing linker defect would result in lower coordination numbers of the Zr atoms and thus higher reactivities, resulting in even lower C-C bond breaking barriers (see Figure S31 for details). The reaction completes through **TS3** (47.8 kcal/mol), returning the Zr node to its initial state and effectively cracking the starting alkane into a terminal alkene and a shorter alkane. Finally, to assess if these transition states were possible within the confinement of the pore cavity of UiO-66, calculations were performed on a larger cage model consisting of two adjacent octahedral pores, and a nonacosane ($C_{29}H_{60}$) strand as a PE surrogate (**Figure 5b**, see Section S6.1 for details). The model shows that the C-C bond breaking transition state is indeed sterically accessible.

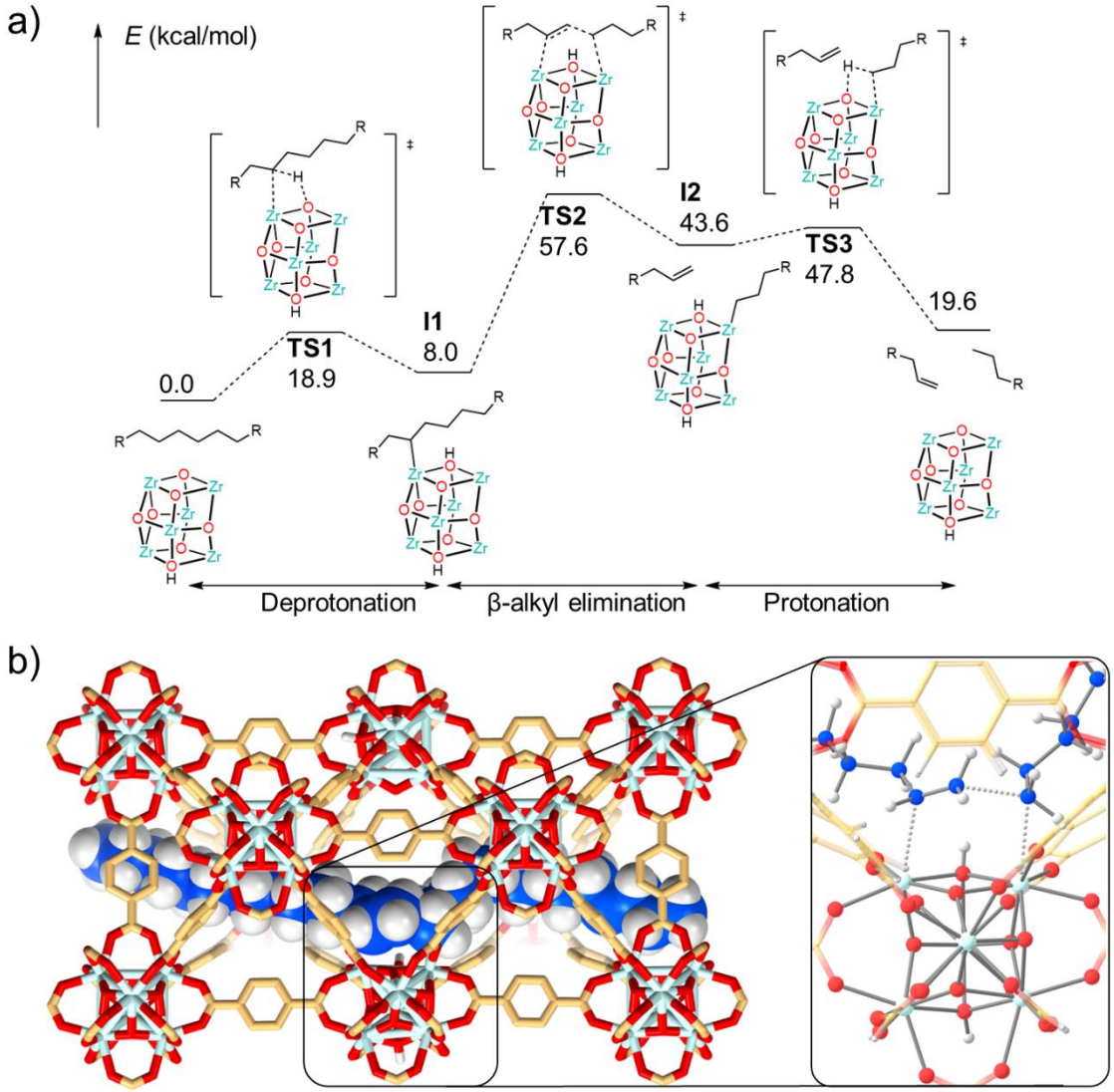

Figure 5 (a) Modelled reaction profile illustrating the C-C bond cleavage catalysed by unsaturated sites on a Zr atom. (b) Computational model illustrating the transition state for bond breaking within a pore of UiO-66. The figure highlights the steric accessibility of polyethylene to the active node. Inset shows an expanded view of the key transition state for bond cleavage.

Conclusion

In summary, we have demonstrated that thermally-stable, low-cost and scalable UiO-66 MOFs can be highly effective catalysts for depolymerization of polyolefin plastic waste under relatively-mild pyrolytic conditions. Under both lab-scale and practical fixed-bed reactor set-ups, UiO-66 significantly enhanced industrially-useful liquid and gas yields from polyolefin substrates, whilst greatly suppressing solid wax formation. Product distribution analyses revealed distinct preferences for alkane and aliphatic olefin formation, providing useful complementarity to the aromatic selectivity typically observed with zeolite catalysts. DSC and solid-state 2D NMR studies indicated the unexpected possibility of polyolefins entering the UiO-66 pores at pyrolytic temperatures, allowing full exploitation of the high MOF internal surface area for reactions catalysed by the coordinatively-unsaturated zirconia nodes. Computational modelling supported the energetic and steric possibility of zirconia-mediated β-alkyl elimination pathways within MOF pores which favour liquid and gas fraction formation over chemical crosslinking that forms solid char. Importantly, the ability of the rigid MOF framework to stabilise and maintain the high reactivity of the nanoparticulate zirconia nodes is essential to their catalytic efficacy, evident from the negligible reactivity of zirconia microparticles observed under identical reaction conditions. Considering that a considerable number of MOFs possess comparable or superior thermal stabilities to UiO-66,[52] with pores sufficiently large for polymer penetration, numerous possibilities for tuning pyrolysis reactivity and product selectivity through bottom-up MOF design can be envisaged. Our study serves as a proof of concept that MOFs, which have been extensively studied for forward polymerization, can also be used effectively for depolymerization, opening up new avenues for future exploitation of these versatile porous materials for waste plastic valorisation.

Supporting Information

The authors have cited additional references within the Supporting Information.[53],[54],[55]

Acknowledgements

The authors acknowledge the UGTO Seed Fund (C211718005) by the Agency for Science, Technology and Research (A*STAR), Singapore for the generous financial support. J.Y.C. Lim is also grateful for financial support from the National Research Foundation (Award number: NRF-NRFF15-2023-0007). S. Kitagawa and K. Otake are grateful for the support from Kyoto University's Overseas On-site Laboratory Program, and the financial support of KAKENHI, Grant-in-Aid for Scientific Research (S) (JP22H05005). This work was supported by the A*STAR Computational Resource Centre through the use of its high performance computing facilities. The synchrotron radiation experiments were performed at beamline BL02B2 and BL36XU of SPring-8.

Keywords: Heterogeneous catalysis • valorisation • polyethylene • polypropylene • hydrocarbons

[1] S. B. Borrelle, J. Ringma, K. L. Law, C. C. Monnahan, L. Lebreton, A. McGivern, E. Murphy, J. Jambeck, G. H. Leonard, M. A. Hilleary et al., *Science* **2020**, *369*, 1515.

[2] R. Geyer, J. R. Jambeck, K. L. Law, *Sci. Adv.* **2017**, *3*, e1700782.

[3] I. Vollmer, M. J. F. Jenks, M. C. P. Roelands, R. J. White, T. van Harmelen, P. de Wild, G. P. van der Laan, F. Meirer, J. T. F. Keurentjes, B. M. Weckhuysen, *Angew. Chem. Int. Ed.* **2020**, *59*, 15402.

[4] a) C. W. S. Yeung, J. Y. Q. Teo, X. J. Loh, J. Y. C. Lim, *ACS Materials Lett.* **2021**, *3*, 1660; b) M. Hong, E. Y.-X. Chen, *Green Chem.* **2017**, *19*, 3692; c) G. W. Coates, Getzler, Yutan D. Y. L., *Nat. Rev. Mater.* **2020**, *5*, 501; d) S. C. Kosloski-Oh, Z. A. Wood, Y. Manjarrez, J. P. de Los Rios, M. E. Fieser, *Mater. Horiz.* **2021**, *8*, 1084; e) J. Y. Q. Teo, A. Ong, T. T. Y. Tan, X. Li, X. J. Loh, J. Y. C. Lim, *Green Chem.* **2022**, *24*, 6086; f) A. Ong, J. Y. Q. Teo, Z. Feng, T. T. Y. Tan, J. Y. C. Lim, *ACS Sustain. Chem. Eng* **2023**, *11*, 12514; g) C. W. S. Yeung, M. H. Periayah, J. Y. Q. Teo, E. T. L. Goh, P. L. Chee, W. W. Loh, X. J. Loh, R. Lakshminarayanan, J. Y. C. Lim, *Macromolecules* **2023**, *56*, 815; h) B.-N. T. Nguyen, J. Y. C. Lim, *Trends Chem.* **2024**, *6*, 100.

[5] V. K. Soni, G. Singh, B. K. Vijayan, A. Chopra, G. S. Kapur, S. S. V. Ramakumar, *Energy Fuels* **2021**, *35*, 12763.

[6] I. Hussain, A. Aitani, Z. Malaibari, H. Alasiri, M. Naseem Akhtar, O. Fahad Aldosari, S. Ahmed, *Chem. Rec.* **2023**, *23*, e202200294.

[7] U. Devi, *The Business Times* **2021**.

[8] H. Li, J. Wu, Z. Jiang, J. Ma, V. M. Zavala, C. R. Landis, M. Mavrikakis, G. W. Huber, *Science* **2023**, *381*, 660.

[9] Z. Xu, N. E. Munyaneza, Q. Zhang, M. Sun, C. Posada, P. Venturo, N. A. Rorrer, J. Miscall, B. G. Sumpter, G. Liu, *Science* **2023**, *381*, 666.

[10] M. Artetxe, G. Lopez, M. Amutio, G. Elordi, J. Bilbao, M. Olazar, *Ind. Eng. Chem. Res.* **2013**, *52*, 10637.

[11] Y. Wang, L. Cheng, J. Gu, Y. Zhang, J. Wu, H. Yuan, Y. Chen, *ACS omega* **2022**, *7*, 2752.

[12] F. Ateş, N. Miskolczi, N. Borsodi, *Bioresour. Technol.* **2013**, *133*, 443.

[13] A. K. Panda, R. K. Singh, D. K. Mishra, *Renew. Sustain. Energy Rev.* **2010**, *14*, 233.

[14] A. Marcilla, M. I. Beltrán, F. Hernández, R. Navarro, *Appl. Catal., A* **2004**, *278*, 37.

[15] J. Aguado, J. L. Sotelo, D. P. Serrano, J. A. Calles, J. M. Escola, *Energy Fuels* **1997**, *11*, 1225.

[16] Z. Dong, W. Chen, K. Xu, Y. Liu, J. Wu, F. Zhang, *ACS Catal.* **2022**, *12*, 14882.

[17] F. D. Cannavacciuolo, R. Yadav, A. Esper, A. Vittoria, G. Antinucci, F. Zaccaria, R. Cipullo, P. H. M. Budzelaar, V. Busico, G. P. Goryunov et al., *Angew. Chem. Int. Ed.* **2022**, *61*, e202202258.

[18] A. Q. Kane, A. M. Esper, K. Searles, C. Ehm, A. S. Veige, *Catal. Sci. Technol.* **2021**, *11*, 6155.

[19] S. Chen, A. Tennakoon, K.-E. You, A. L. Paterson, R. Yappert, S. Alayoglu, L. Fang, X. Wu, T. Y. Zhao, M. P. Lapak et al., *Nat. Catal.* **2023**, *6*, 161.

[20] V. Dufaud, J.-M. Basset, *Angew. Chem. Int. Ed.* **1998**, *37*, 806.

[21] C. Lecuyer, F. Quignard, A. Choplin, D. Olivier, J.-M. Basset, *Angew. Chem. Int. Ed. Engl.* **1991**, *30*, 1660.

[22] A. H. Mason, A. Motta, A. Das, Q. Ma, M. J. Bedzyk, Y. Kratish, T. J. Marks, *Nat Commun* **2022**, *13*, 7187.

[23] A. Corma, *Chem. Rev.* **1995**, *95*, 559.

[24] X. Feng, H. S. Jena, C. Krishnaraj, K. Leus, G. Wang, H. Chen, C. Jia, P. van der Voort, *ACS Appl. Mater. Interfaces* **2021**, *13*, 60715.

[25] T. A. Goetjen, J. Liu, Y. Wu, J. Sui, X. Zhang, J. T. Hupp, O. K. Farha, *Chem. Commun.* **2020**, *56*, 10409.

[26] R. C. Klet, S. Tussupbayev, J. Borycz, J. R. Gallagher, M. M. Stalzer, J. T. Miller, L. Gagliardi, J. T. Hupp, T. J. Marks, C. J. Cramer et al., *J. Am. Chem. Soc.* **2015**, *137*, 15680.

[27] P. Ji, J. B. Solomon, Z. Lin, A. M. Wilders, R. F. Jordan, W. Lin, *J. Am. Chem. Soc.* **2017**, *139*, 11325.

[28] T. Uemura, N. Yanai, S. Kitagawa, *Chem. Soc. Rev.* **2009**, *38*, 1228.

[29] a) J. Heng, T. Tan, Z. Xing, J. Ong, K. S. Lin, X. Q. Koh, W. Jiang, L. Zhang, Q. Zhu, Z. Li et al., *Mater. Today Chem.* **2023**, *31*, 101608; b) R. Mishra, A. Kumar, E. Singh, S. Kumar, *ACS Sustain. Chem. Eng* **2023**, *11*, 2033.

[30] O. M. Yaghi, M. O'Keeffe, N. W. Ockwig, H. K. Chae, M. Eddaoudi, J. Kim, *Nature* **2003**, *423*, 705.

[31] C. Healy, K. M. Patil, B. H. Wilson, L. Hermanspahn, N. C. Harvey-Reid, B. I. Howard, C. Kleinjan, J. Kolien, F. Payet, S. G. Telfer et al., *Coord. Chem. Rev.* **2020**, *419*, 213388.

[32] T. Kitao, Y. Zhang, S. Kitagawa, B. Wang, T. Uemura, *Chem. Soc. Rev.* **2017**, *46*, 3108.

[33] a) P. Duan, J. C. Moreton, S. R. Tavares, R. Semino, G. Maurin, S. M. Cohen, K. Schmidt-Rohr, *J. Am. Chem. Soc.* **2019**, *141*, 7589; b) T. Uemura, N. Yanai, S. Watanabe, H. Tanaka, R. Numaguchi, M. T. Miyahara, Y. Ohta, M. Nagaoka, S. Kitagawa, *Nat Commun* **2010**, *1*, 83.

[34] B. Le Ouay, C. Watanabe, S. Mochizuki, M. Takayanagi, M. Nagaoka, T. Kitao, T. Uemura, *Nat. Commun.* **2018**, *9*, 3635.

[35] S. Yang, V. V. Karve, A. Justin, I. Kochetygov, J. Espín, M. Asgari, O. Trukhina, D. T. Sun, L. Peng, W. L. Queen, *Coord. Chem. Rev.* **2021**, *427*, 213525.

[36] Y. Wu, X. Wang, K. O. Kirlikovali, X. Gong, A. Atilgan, K. Ma, N. M. Schweitzer, N. C. Gianneschi, Z. Li, X. Zhang et al., *Angew. Chem. Int. Ed.* **2022**, *61*, e202117528.

[37] M. Chauhan, N. Antil, B. Rana, N. Akhtar, C. Thadhani, W. Begum, K. Manna, *JACS Au* **2023**, *3*, 3473.

[38] S. Øien, D. Wragg, H. Reinsch, S. Svelle, S. Bordiga, C. Lamberti, K. P. Lillerud, *Cryst. Growth Des.* **2014**, *14*, 5370.

[39] J. H. Cavka, S. Jakobsen, U. Olsbye, N. Guillou, C. Lamberti, S. Bordiga, K. P. Lillerud, *J. Am. Chem. Soc.* **2008**, *130*, 13850.

[40] J. Hajek, B. Bueken, M. Waroquier, D. de Vos, V. van Speybroeck, *ChemCatChem* **2017**, *9*, 2203.

[41] M. J. Katz, Z. J. Brown, Y. J. Colón, P. W. Siu, K. A. Scheidt, R. Q. Snurr, J. T. Hupp, O. K. Farha, *Chem. Commun.* **2013**, *49*, 9449.

[42] G. C. Shearer, S. Chavan, S. Bordiga, S. Svelle, U. Olsbye, K. P. Lillerud, *Chem. Mater.* **2016**, *28*, 3749.

[43] A. Aboulkas, K. El harfi, A. El Bouadili, *Energy Convers. Manag.* **2010**, *51*, 1363.

[44] G. C. Shearer, S. Chavan, J. Ethiraj, J. G. Vitillo, S. Svelle, U. Olsbye, C. Lamberti, S. Bordiga, K. P. Lillerud, *Chem. Mater.* **2014**, *26*, 4068.

[45] A. T. Jones, J. M. Aizlewood, D. R. Beckett, *Makromol. Chem.* **1964**, *75*, 134.

[46] K. Schmidt-Rohr, H.W. Spiess, *Multidimensional Solid-State NMR and Polymers*, Academic Press, **1994**.

[47] a) J. M. D. Lane, N. W. Moore, *J. Phys. Chem. A* **2018**, *122*, 3962; b) K. V. Popov, V. D. Knyazev, *J. Phys. Chem. A* **2015**, *119*, 11737.

[48] M. L. Poutsma, *Macromolecules* **2003**, *36*, 8931.

[49] K. Tanaka, M. Takakura, Y. Koshino, *J. Appl. Polym. Sci.* **1974**, *18*, 1131.

[50] a) F. Neese, *WIREs Comput Mol Sci* **2022**, *12*; b) F. Neese, *WIREs Comput Mol Sci* **2012**, *2*, 73.

[51] V. D. Knyazev, *J. Phys. Chem. A* **2007**, *111*, 3875.

[52] C. Healy, K. M. Patil, B. H. Wilson, L. Hermanspahn, N. C. Harvey-Reid, B. I. Howard, C. Kleinjan, J. Kolien, F. Payet, S. G. Telfer et al., *Coord. Chem. Rev.* **2020**, *419*, 213388.

[53] a) K. Saalwächter, F. Lange, K. Matyjaszewski, C.-F. Huang, R. Graf, *J. Magn. Reson.* **2011**, *212*, 204; b) D. Marion, M. Ikura, R. Tschudin, A. Bax, *J. Magn. Reson.* **1989**, *85*, 393.

[54] a) T. Uruga, M. Tada, O. Sekizawa, Y. Takagi, T. Yokoyama, Y. Iwasawa, *Chem. Rec.* **2019**, *19*, 1444; b) B. Ravel, M. Newville, *J. Synchrotron Radiat.* **2005**, *12*, 537.

[55] a) L. W. Chung, H. Hirao, X. Li, K. Morokuma, *WIREs Comput Mol Sci* **2012**, *2*, 327; b) C. Plett, A. Katbashev, S. Ehlert, S. Grimme, M. Bursch, *Phys. Chem. Chem. Phys.* **2023**, *25*, 17860; c) D. Andrae, U. Huermann, M. Dolg, H. Stoll, H. Preu, *Theoret. Chim. Acta* **1990**, *77*, 123; d) S. Grimme, J. Antony, S. Ehrlich, H. Krieg, *J. Chem. Phys.* **2010**, *132*, 154104; e) Perdew, Burke, Ernzerhof, *Phys. Rev. Lett.* **1996**, *77*, 3865; f) F. Weigend, *Phys. Chem. Chem. Phys.* **2006**, *8*, 1057; g) F. Weigend, R. Ahlrichs, *Phys. Chem. Chem. Phys.* **2005**, *7*, 3297; h) S. Grimme, C. Bannwarth, P. Shushkov, *J. Chem. Theory. Comput.* **2017**, *13*, 1989; i) V. Barone, M. Cossi, *J. Phys. Chem. A* **1998**, *102*, 1995.

Entry for the Table of Contents

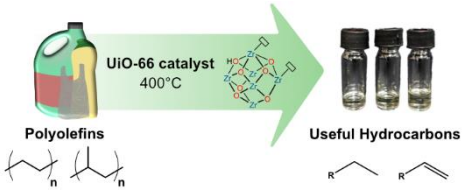

Defective UiO-66, a Zr-based metal-organic framework (MOF) catalyst, overcomes limitations in plastic waste depolymerization. During pyrolysis at 400 °C, it promotes conversion of polyolefins to useful liquid and gaseous hydrocarbons, reducing solid wax formation. This approach also offers a distinct catalytic pathway compared to conventional zeolite catalysts.

Institute and/or researcher Twitter usernames: ((optional))